

First Measurement of the Q^2 Dependence of the Beam-Normal Single Spin Asymmetry for Elastic Scattering off Carbon

A. Esser, M. Thiel, P. Achenbach, K. Aulenbacher, S. Baunack, J. Beričič, D. Bosnar, L. Correa, M. Dehn, M.O. Distler, et al.

► **To cite this version:**

A. Esser, M. Thiel, P. Achenbach, K. Aulenbacher, S. Baunack, et al.. First Measurement of the Q^2 Dependence of the Beam-Normal Single Spin Asymmetry for Elastic Scattering off Carbon. Phys.Rev.Lett., 2018, 121 (2), pp.022503. 10.1103/PhysRevLett.121.022503 . hal-01851161

HAL Id: hal-01851161

<https://hal.archives-ouvertes.fr/hal-01851161>

Submitted on 9 May 2019

HAL is a multi-disciplinary open access archive for the deposit and dissemination of scientific research documents, whether they are published or not. The documents may come from teaching and research institutions in France or abroad, or from public or private research centers.

L'archive ouverte pluridisciplinaire **HAL**, est destinée au dépôt et à la diffusion de documents scientifiques de niveau recherche, publiés ou non, émanant des établissements d'enseignement et de recherche français ou étrangers, des laboratoires publics ou privés.

First Measurement of the Q^2 -dependence of the Beam-Normal Single Spin Asymmetry for Elastic Scattering off Carbon

A. Esser,¹ M. Thiel,^{1,*} P. Achenbach,¹ K. Aulenbacher,¹ S. Baunack,¹ J. Beričič,² D. Bosnar,³ L. Correa,⁴ M. Dehn,¹ M. O. Distler,¹ H. Fonvieille,⁴ I. Friščić,^{3,†} M. Gorchtein,¹ S. Heidrich,¹ P. Herrmann,¹ M. Hoek,¹ S. Kegel,¹ Y. Kohl,¹ T. Kolar,^{5,2} H.-J. Kreidel,¹ F. E. Maas,¹ H. Merkel,¹ M. Mihovilović,^{1,2} J. Müller,¹ U. Müller,¹ F. Nillius,¹ C. Palatchi,⁶ K. D. Paschke,⁶ J. Pochodzalla,¹ B. S. Schlimme,¹ M. Schoth,¹ F. Schulz,¹ S. Širca,^{5,2} B. Spruck,¹ S. Štajner,² V. Tioukine,¹ A. Tyukin,¹ A. Weber,¹ and C. Sienti¹

¹*Institut für Kernphysik, Johannes Gutenberg-Universität Mainz, D-55099 Mainz, Germany*

²*Jožef Stefan Institute, SI-1000 Ljubljana, Slovenia*

³*Department of Physics, Faculty of Science, University of Zagreb, 10000 Zagreb, Croatia*

⁴*Clermont Université, Université Blaise Pascal, CNRS/IN2P3, LPC, BP 10448, F-63000 Clermont-Ferrand, France*

⁵*Department of Physics, University of Ljubljana, SI-1000 Ljubljana, Slovenia*

⁶*University of Virginia, Charlottesville, Virginia 22903, USA*

We report on the first Q^2 -dependent measurement of the beam-normal single spin asymmetry A_n in the elastic scattering of 570 MeV vertically polarized electrons off ^{12}C . We covered the Q^2 range between 0.02 and 0.05 GeV^2/c^2 and determined A_n at four different Q^2 values. The experimental results are compared to a theoretical calculation that relates A_n to the imaginary part of the two-photon exchange amplitude. The result emphasizes that the Q^2 -behaviour of A_n given by the ratio of the Compton to charge form factors cannot be treated independently of the target nucleus.

PACS numbers: 13.40.-f, 25.30.Bf, 27.20.+n

Over the last 60 years electron scattering experiments with ever increasing precision offer manifold opportunities to study the structure of nuclei. The technological progress nowadays allows to perform parity-violating electron scattering experiments [1] with statistical and systematic errors better than one part per billion (ppb). Such experiments at the precision frontier enable measurements of the strangeness contribution to the vector form factors of the proton [2–4], the weak charge of the proton and the weak mixing angle θ_W [5–7] as well as the neutron-skin thickness of heavy nuclei [8]. Moreover, driven by recent theoretical predictions new experiments are planned to determine parity-violating asymmetries as a portal to physics beyond the Standard Model [9, and references therein]. Two boson exchange corrections play a major role in interpreting many experiments at the precision frontier, but represent a considerable difficulty theoretically. Such is the case with the γZ -box in PVES [10], the γW -box in nuclear β -decays [11], and the 2γ -box in the form-factor measurements [12]. Dispersion relations have established themselves as the main tool for such calculations. The imaginary part of the two boson exchange diagram serves as input in these calculations, so a direct measurement of this imaginary part provides a valuable test of theoretical calculations. Experimentally, the imaginary (absorptive) part of the two-photon exchange amplitude can be accessed through the beam-normal single spin asymmetry (or so-called transverse asymmetry) A_n in elastic scattering of electrons polarized perpendicular to the scattering plane off unpolarized nucleons. The transverse asymmetry arises from the interference of the one-photon and two-photon exchange

amplitudes [13] and is defined as

$$A_n = \frac{\sigma_{\uparrow} - \sigma_{\downarrow}}{\sigma_{\uparrow} + \sigma_{\downarrow}}, \quad (1)$$

where σ_{\uparrow} (σ_{\downarrow}) represents the cross section for the elastic scattering of electrons with spin vector \vec{P}_e parallel (antiparallel) to the normal vector, defined by $\hat{n} = (\vec{k} \times \vec{k}')/|\vec{k} \times \vec{k}'|$. \vec{k} and \vec{k}' are the three-momenta of the incident and scattered electron, respectively. The experimentally measured asymmetry A_{exp} is related to A_n by

$$A_{\text{exp}} = A_n \vec{P}_e \cdot \hat{n}. \quad (2)$$

The calculations for the theoretical treatment of two-photon exchange processes in general kinematics are challenging because they require an account of inclusive hadronic intermediate states with arbitrary virtualities of the exchanged photons. By considering only the very low momentum transfer region ($m_e c \ll Q \ll E/c$), where the leading order is $\sim C_0 \cdot \log(Q^2/m_e^2 c^2)$, this complication is alleviated [14, 15]. Since the coefficient C_0 is obtained in a model-independent way from the optical theorem as an energy-weighted integral over the total photoabsorption cross-section on the particular target, this expression can be calculated exactly.

Calculations of A_n for the reaction $p(\vec{e}, e')p$ using this inclusive approach [14, 15], as well as models with a partial account of the excited hadronic spectrum [16, 17] provide a good description of forward scattering data [18] and reasonably good description of large scattering angle data [19–22] with the exception of the backward scattering data of Ref. [23]. Gorchtein and Horowitz [24] gener-

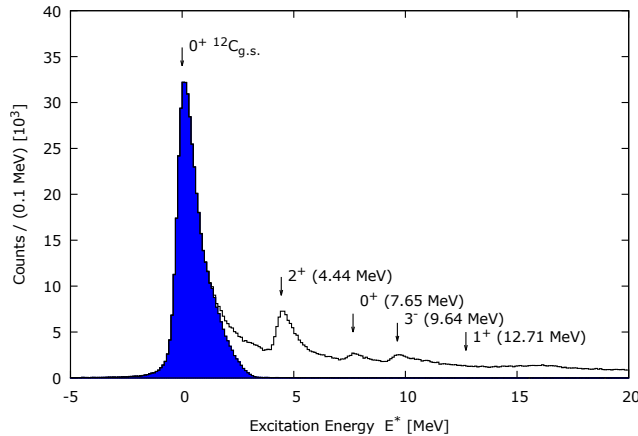


FIG. 1. (color online). The excitation energy spectrum shows the acceptance of the spectrometer without Cherenkov cut (black line) and of the Cherenkov detector only (filled area). By changing the magnetic field of the spectrometer the elastic peak was moved until it matched the position of the Cherenkov detector.

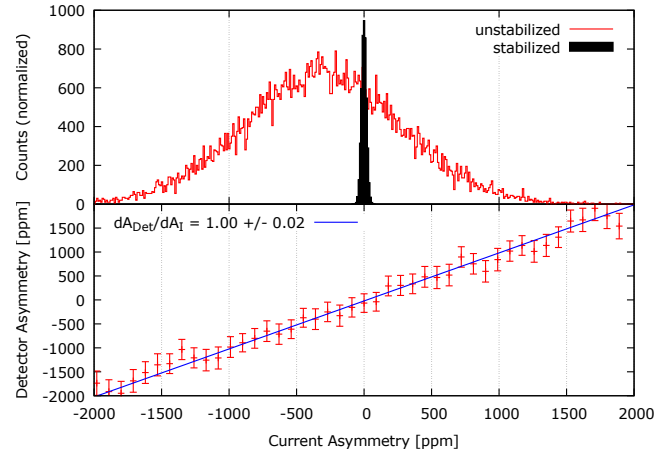


FIG. 2. (color online). *Top*: Comparison between the asymmetry in the integrated signal from a beam current monitor observed in a run with beam stabilization off (red) and with beam stabilization on (black). *Bottom*: Raw asymmetry determined for one PMT of the Cherenkov detector in spectrometer B as a function of the current asymmetry for a run without beam stabilization.

79 alized the forward inclusive model to nuclear targets

$$A_n \sim C_0 \cdot \log\left(\frac{Q^2}{m_e^2 c^2}\right) \cdot \frac{F_{\text{Compton}}(Q^2)}{F_{\text{ch}}(Q^2)}. \quad (3)$$

80 For the Compton slope parameter only data for the pro-
81 ton and for ^4He are available, suggesting that the relevant
82 Q^2 -behaviour for A_n given by the ratio of the Compton
83 to charge form factors

$$\frac{F_{\text{Compton}}(Q^2)}{F_{\text{ch}}(Q^2)} \approx \exp[-4Q^2/(\text{GeV}^2/c^2)] \quad (4)$$

84 is roughly independent of the target. The calculation
85 was compared to forward scattering data ($\theta \leq 6^\circ$)
86 taken at the Jefferson Laboratory on ^1H , ^4He , ^{12}C , and
87 ^{208}Pb [18]: while the calculation is in good agreement
88 with the observed asymmetries for lighter targets, it
89 failed completely to reproduce the ^{208}Pb data. This
90 has a major impact on parity-violating electron scat-
91 tering experiments, since the transverse asymmetry,
92 arising from a non-zero vertical component of the
93 beam polarization, produces false asymmetries that
94 contribute substantially to the total systematic error.
95 This contribution will become even more crucial for
96 future experiments [9, 25] aiming at a precision much
97 higher than ever attained before. Systematic studies
98 of A_n dependencies on the momentum transfer, the
99 nuclear charge and the energy are absolutely mandatory
100 to benchmark the current theoretical description of
101 A_n , thus providing also new insight into the structure
102 of nuclei. The aim of our measurement is to perform
103 the first systematic study of the Q^2 -dependence of the
104 beam-normal single spin asymmetry for light nuclei.
105 The experiment was performed at the spectrometer

109 setup of the A1 Collaboration at the Mainz Microtron
110 MAMI [26]. The polarized 570 MeV electrons were
111 produced using a strained GaAs/GaAsP super lattice
112 photocathode that was irradiated with circularly po-
113 larized laser light [27, 28]. The longitudinal spin of
114 the electrons leaving the photocathode was rotated to
115 transverse orientation (in the horizontal plane) using
116 a Wien filter which is positioned between the 100 keV
117 polarized electron source and the injector linac of the
118 accelerator. The polarization vector was finally rotated
119 to vertical orientation using a pair of solenoids, located
120 shortly behind the Wien filter. The orientation of
121 the electron beam polarization vector was alternating
122 between up and down by setting the high voltage of a
123 fast Pockels cell in the optical system of the polarized
124 electron source. The orientation as well as the degree of
125 the polarization have been determined and monitored
126 during the whole measuring campaign [29]. This was
127 accomplished using a Mott polarimeter [30] downstream
128 of the 3.5 MeV injector linac and a Møller polarimeter
129 [31] close to the interaction point in the spectrome-
130 ter hall. The degree of the vertical polarization was
131 deduced by subtracting the horizontal polarization
132 components from the total polarization and was on
133 average $P_e = 82.7\% \pm 0.3\%(\text{stat.}) \pm 1.1\%(\text{syst.})$.
134 For the measurement of the beam-normal single spin
135 asymmetry A_n a 20 μA continuous-wave beam of
136 vertically polarized electrons was impinging on a 2.27
137 g/cm^2 carbon target. Elastically scattered electrons
138 were focused onto two fused silica detectors positioned in
139 the focal plane of the two high-resolution spectrometers
140 A and B of the A1 setup [32], located to the left and

TABLE I. Measured beam-normal single spin asymmetries for each spectrometer and kinematical setting with the corresponding statistical and systematic uncertainty contributions in units of parts per million (ppm).

Spectrometer	B	B	B	A	A
Setup	3	2	1	1	2&3
Q^2 (GeV^2/c^2)	0.023	0.030	0.041	0.039	0.049
A_n	-15.984	-20.672	-21.933	-23.877	-28.296
Energy fluctuation δE	0.007	0.006	0.009	0.009	0.001
Current asymmetry δI	0.013	0.015	0.011	0.011	0.010
Vertical beam position δy	0.003	0.001	0.005	0.005	0.002
Horizontal beam position δx	0.001	0.003	0.005	0.023	0.012
Vertical angle $\delta y'$	0	0	0	0	0
Horizontal angle $\delta x'$	0.003	0.001	0.001	0.001	0.001
Gate length	0.013	0.010	0.010	0.010	0.008
P_e measurement	0.245	0.385	0.480	0.523	0.491
PMT gain variation	0.380	0.130	1.100	0.170	0.030
Total systematic error	0.664	0.551	1.621	0.752	0.555
Statistical error	1.061	0.959	1.515	0.967	1.372

141 right side of the incoming beam, respectively. The fused
 142 silica detectors were oriented at 45° with respect to
 143 the direction of the electrons in the spectrometer. The
 144 sizes of the two fused silica bars ($(300 \times 70 \times 10)$ mm³
 145 and $(100 \times 70 \times 10)$ mm³) were chosen according to the
 146 different focal plane geometries of the two spectrometers.
 147 The produced Cherenkov light was detected by 25 mm
 148 fused silica-window photomultipliers directly attached to
 149 the fused silica bars: five for the detector in spectrometer
 150 A and three for the detector in spectrometer B.
 151 To reach a sufficiently high count rate, the detec-
 152 tors had to be placed in the most forward direction.
 153 Limited by the distance between the exit beam line
 154 and its quadrupole, spectrometer A was placed at
 155 its minimum angle of 23.50° which corresponds to
 156 $Q^2 = 0.04 \text{ GeV}^2/c^2$, at a beam energy of 570 MeV. In
 157 accordance with its smaller focal plane, spectrometer B
 158 was placed at 20.61° to cover the same momentum range.
 159 This measurement allowed for identification of possible
 160 false asymmetries due to helicity correlated changes
 161 of the beam parameters. With this configuration the
 162 extracted asymmetries for each spectrometer were equal
 163 within the experimental uncertainties (see Fig. 3), thus
 164 confirming a negligible contribution to beam-related false
 165 asymmetries. Therefore three more Q^2 measurements
 166 were performed during the same experiment by changing
 167 the kinematical configuration of the spectrometers:
 168 one measurement at $Q^2 = 0.05 \text{ GeV}^2/c^2$ by placing
 169 spectrometer A at 25.90° and two more measurements at
 170 $Q^2 = 0.03 \text{ GeV}^2/c^2$ and $Q^2 = 0.02 \text{ GeV}^2/c^2$ by placing
 171 spectrometer B at 17.65° and 15.11° , respectively.
 172 During the experiment, the fused silica detectors were
 173 operated in two different modes. The position of the
 174 Cherenkov detectors within the elastic line was opti-
 175 mized during the low current mode ($I = 50 \text{ nA}$). For

176 this purpose the fused silica detectors were read out
 177 in coincidence with the vertical drift-chambers of the
 178 spectrometers. The obtained excitation energy spectrum
 179 shown in Fig. 1 demonstrates the clear separation
 180 between elastic and inelastic events from the first excited
 181 state of carbon at 4.4 MeV.
 182 In the high current (or integrating) mode the ampli-
 183 fication of the PMTs was reduced from nominal to
 184 avoid a non-linear behaviour. While all other detector
 185 components of the spectrometers were switched off
 186 to prevent additional noise, the fused silica detectors
 187 were read out with parts of the former A4 experiment
 188 data acquisition system [2]. The response of each PMT
 189 was recorded with an ADC, integrating the charge
 190 over periods of 20 ms. A gate generator provided the
 191 integration windows where the polarization is reversed
 192 in patterns like $\uparrow \downarrow \downarrow \uparrow$ or $\downarrow \uparrow \uparrow \downarrow$ in a pseudo random
 193 sequence. Moreover, an additional $\lambda/2$ -wave plate was
 194 periodically inserted in the laser system of the source
 195 to identify possible false asymmetries and to suppress
 196 many systematic effects.
 197 In order to minimize helicity-correlated beam-
 198 fluctuations, four dedicated stabilization systems
 199 (beam current, beam energy, slow position (DC), and
 200 fast position (AC)) were used at MAMI. The beam
 201 parameters were measured by several monitors, placed
 202 in the A1 beamline, which were read out together with
 203 the detector signals. As an example, Fig. 2 (top panel)
 204 shows the impact of the beam current stabilization
 205 system on the current asymmetry.
 206 Moreover, calibration runs over the full beam current
 207 range as well as in a narrow region around $20 \mu\text{A}$ were
 208 performed regularly to monitor the functioning and the
 209 linearity of the PMTs.

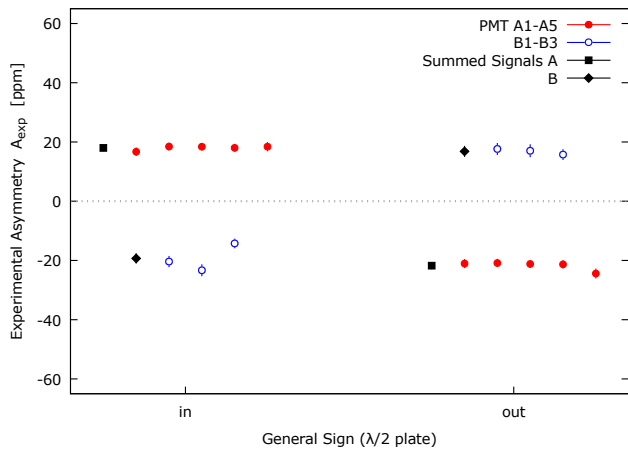


FIG. 3. (color online). The transverse asymmetry A_{exp} for each PMT of the detectors placed in spectrometer A (filled red circles) and spectrometer B (open blue circles) at $Q^2 = 0.04 \text{ GeV}^2/c^2$. By inserting an additional $\lambda/2$ -wave plate into the laser beam of the polarized electron source, the general sign changed.

210 We calculate the raw detector asymmetry A_{raw} as

$$A_{\text{raw}} = \frac{N_e^\uparrow - N_e^\downarrow}{N_e^\uparrow + N_e^\downarrow}, \quad (5)$$

211 where $N_e^{\uparrow(\downarrow)}$ denotes the integrated detector signal which
 212 is proportional to the detected number of elastically scat-
 213 tered electrons for each polarization state. Even though
 214 with our dedicated stabilization systems helicity corre-
 215 lated changes of the beam parameters were suppressed as
 216 well as possible, tiny remnants can always lead to false
 217 asymmetries. Therefore, correction factors c_i ($i = 1..6$)
 218 were applied to the beam current asymmetry A_I , the
 219 horizontal and vertical beam position differences Δx and
 220 Δy , the horizontal and vertical beam angle differences
 221 $\Delta x'$ and $\Delta y'$, and the beam energy difference ΔE to de-
 222 termine the experimental asymmetry

$$A_{\text{exp}} = A_{\text{raw}} - c_1 A_I - c_2 \Delta x - c_3 \Delta y - c_4 \Delta x' - c_5 \Delta y' - c_6 \Delta E. \quad (6)$$

223 Typically, the correction factors would be derived from a
 225 multidimensional regression of the measured asymmetry
 226 versus the corresponding parameters. However, due to
 227 the extraordinary high-quality beam during the experi-
 228 mental campaign, the variation of the parameters was too
 229 narrow compared to the width of the asymmetry to ap-
 230 ply this method. Instead, analytical calculations as well
 231 as simulations were used to determine the individual cor-
 232 rection factors. The factor c_1 in Eq. 6 must be equal to
 233 one, since the luminosity changes linearly with the beam
 234 current. This correlation has been verified in runs taken
 235 without the beam-current stabilization system as illus-
 236 trated in Fig. 2 (bottom panel). The factors c_2 and c_3
 237 for position related false asymmetries were estimated by

238 using Monte-Carlo simulations. In addition, a small data
 239 sample acquired without beam stabilizations was used
 240 as a cross-check and both results were in good agree-
 241 ment. Concerning the beam angle differences, an ana-
 242 lytical derivation of a parametrization of the Mott cross-
 243 section was used to determine the correction factor c_4 for
 244 the horizontal scattering angle. The correction factor c_5
 245 for the vertical scattering angle vanishes since the angu-
 246 lar acceptance of both spectrometers is symmetric with
 247 respect to their bending planes. Nevertheless, variations
 248 of the vertical scattering angle will cause changes of the
 249 effective degree of polarization by up to 1%. This effect
 250 could be corrected by using the position information from
 251 the vertical drift-chambers obtained during the low cur-
 252 rent mode. Since the sign of the energy fluctuation vari-
 253 ation is unknown, no corrections could be applied in this
 254 case. Therefore it has been treated as contribution to the
 255 systematic error. Besides the beam related systematic
 256 uncertainties, the major contribution to the total system-
 257 atic error comes from the aging of the PMTs which re-
 258 sults in a reduction of gain and subsequent non-linearity,
 259 especially when running at high count rates. The rela-
 260 tionship between a given PMTs gain reduction and its
 261 corresponding non-linearity was studied with frequently
 262 performed calibration runs, post-experiment. Retroac-
 263 tive corrections ($0.064 \text{ ppm} < c_{\text{PMT}} < 0.588 \text{ ppm}$) were
 264 applied to the data based on gain degradation. The
 265 larger corrections for the setups B1 and B3 are due to
 266 the gain of the voltage dividers which was set too high
 267 and the high count rate, respectively. Furthermore, cur-
 268 rent unstabilized runs were taken intermittently during
 269 the run period. These runs were used to estimate the
 270 dA/dI deviation from unity (Fig. 2, bottom panel) and
 271 to characterize the degree of non-linearity which had de-
 272 veloped in each PMT. The individual contributions to
 273 the total systematic uncertainty are summarized in Ta-
 274 ble I.

276 To confirm the feasibility of the experimental method and
 277 the analysis procedure as well, the experimental asym-
 278 metry A_{exp} was first extracted for setup 1 (see Table I)
 279 where both spectrometers covered the same momentum
 280 range. Figure 3 shows the measured A_{exp} in each spec-
 281 trometer and for each PMT. The asymmetries obtained
 282 with both detector systems were, as expected, similar
 283 in magnitude but of opposite sign, since \hat{n} in Eq. 2 re-
 284 verses sign. In addition, it can be seen that also the sign
 285 of the asymmetry consistently changed when the addi-
 286 tional $\lambda/2$ -wave plate was moved into the laser beam of
 287 the polarized electron source.

288 Finally, the experimental asymmetry A_{exp} was normal-
 289 ized to the electron beam polarization to extract the
 290 physics asymmetry A_n . The experimentally determined
 291 values for all four kinematic configurations and the cor-
 292 responding statistical and systematic uncertainties are
 293 summarized in Table I. For illustration the data is shown
 294 in Fig. 4. The curve represents the leading Q^2 behaviour

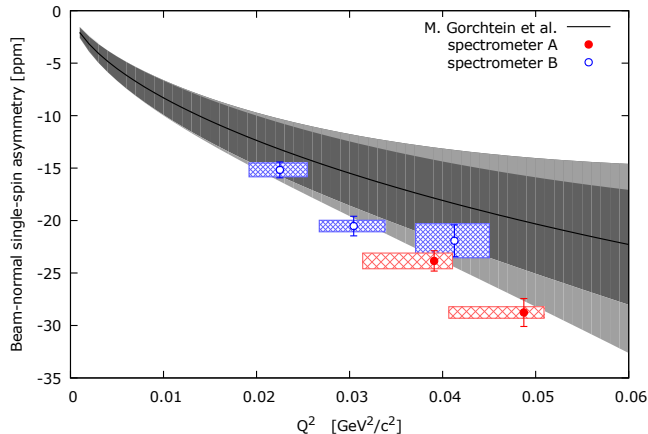


FIG. 4. (color online). Extracted transverse asymmetries A_n for the detectors placed in spectrometer A (filled red circles) and spectrometer B (open blue circles) versus Q^2 . The width of the given boxes indicates the full width at half maximum of the Q^2 distribution which is determined by the intersection of the angular acceptance of the spectrometers and the geometry of the detectors. The statistical and systematic uncertainties are given by the error bars and the height of the boxes, respectively. The theoretical calculation of Ref. [24] (black line) is shown for comparison. The given bands belong to the uncertainty of the Compton slope parameter of 10% (dark grey) and 20% (light grey).

as calculated in the model of Ref. [24] upon neglecting corrections $\sim Q^2/E^2$. The given uncertainty of the theoretical prediction is obtained from two sources: the Compton slope parameter for the ^{12}C target and terms not enhanced by the large logarithm (see [24] for details). The two are expected to be independent and are added in quadrature. The Compton slope parameter introduced in Eq. 4 was allowed to vary within 10% and 20% of the central value, corresponding to the inner and outer band shown in Fig. 4. The comparison of the data with the model indicates that the assumption of the dominance of the $\log(Q^2/m_e^2 c^2)$ term and the independence of $F_{\text{Compton}}(Q^2)/F_{\text{ch}}(Q^2)$ of the target nucleus in Eq. 4, successfully describing ^1H and ^4He data, reproduces the ^{12}C data only within a 20% uncertainty. Even larger deviations could be expected for heavier nuclei.

Future measurements at MAMI will investigate the transverse asymmetry for heavier nuclei at the same Q^2 values. This will serve, together with the current data set, as an important input for future theoretical calculations to achieve a better control of the two-photon exchange mechanism and they might contribute to a deeper understanding of the structure of nuclei.

We acknowledge the MAMI accelerator group and all the workshop staff members for outstanding support. We thank Krishna Kumar for many stimulating discussions and valuable suggestions in the preparation of the experiment. This work was supported by the PRISMA (Preci-

sion Physics, Fundamental Interactions and Structure of Matter) Cluster of Excellence, the Deutsche Forschungsgemeinschaft through the Collaborative Research Center 1044 and the Federal State of Rhineland-Palatinate.

* thielm@uni-mainz.de

† Present address: MIT-LNS, Cambridge MA, 02139, USA

- [1] D. H. Beck and R. D. McKeown, *Ann. Rev. Nucl. Part. Sci.* **51**, 189 (2001), arXiv:hep-ph/0102334 [hep-ph].
- [2] F. E. Maas *et al.* (A4), *Phys. Rev. Lett.* **93**, 022002 (2004), arXiv:nucl-ex/0401019 [nucl-ex].
- [3] D. S. Armstrong *et al.* (G0), *Phys. Rev. Lett.* **95**, 092001 (2005), arXiv:nucl-ex/0506021 [nucl-ex].
- [4] K. A. Aniol *et al.* (HAPPEX), *Phys. Lett.* **B635**, 275 (2006), arXiv:nucl-ex/0506011 [nucl-ex].
- [5] P. L. Anthony *et al.* (SLAC E158), *Phys. Rev. Lett.* **95**, 081601 (2005), arXiv:hep-ex/0504049 [hep-ex].
- [6] D. Androic *et al.* (Qweak), *Phys. Rev. Lett.* **111**, 141803 (2013), arXiv:1307.5275 [nucl-ex].
- [7] D. Androic *et al.* (Qweak), *Nature* **557**, 207 (2018).
- [8] S. Abrahamyan *et al.*, *Phys. Rev. Lett.* **108**, 112502 (2012), arXiv:1201.2568 [nucl-ex].
- [9] D. Becker *et al.*, (2018), arXiv:1802.04759 [nucl-ex].
- [10] M. Gorchtein, C. J. Horowitz, and M. J. Ramsey-Musolf, *Phys. Rev.* **C84**, 015502 (2011), arXiv:1102.3910 [nucl-th].
- [11] W. J. Marciano and A. Sirlin, *Phys. Rev. Lett.* **96**, 032002 (2006), arXiv:hep-ph/0510099 [hep-ph].
- [12] A. Afanasev, P. G. Blunden, D. Hasell, and B. A. Raue, *Prog. Part. Nucl. Phys.* **95**, 245 (2017), arXiv:1703.03874 [nucl-ex].
- [13] A. De Rujula, J. M. Kaplan, and E. De Rafael, *Nucl. Phys.* **B35**, 365 (1971).
- [14] A. V. Afanasev and N. P. Merenkov, *Phys. Lett.* **B599**, 48 (2004), arXiv:hep-ph/0407167 [hep-ph].
- [15] M. Gorchtein, *Phys. Rev.* **C73**, 035213 (2006), arXiv:hep-ph/0512106 [hep-ph].
- [16] B. Pasquini and M. Vanderhaeghen, *Proceedings, 2nd International Workshop on From parity violation to hadronic structure and more (PAVI 2004): Grenoble, France, June 8-11, 2004*, *Eur. Phys. J. A* **24S2**, 29 (2005), [,29(2005)], arXiv:hep-ph/0502144 [hep-ph].
- [17] B. Pasquini and M. Vanderhaeghen, *Phys. Rev.* **C70**, 045206 (2004), arXiv:hep-ph/0405303 [hep-ph].
- [18] S. Abrahamyan *et al.* (HAPPEX, PREX), *Phys. Rev. Lett.* **109**, 192501 (2012), arXiv:1208.6164 [nucl-ex].
- [19] F. E. Maas *et al.*, *Phys. Rev. Lett.* **94**, 082001 (2005), arXiv:nucl-ex/0410013 [nucl-ex].
- [20] D. S. Armstrong *et al.* (G0), *Phys. Rev. Lett.* **99**, 092301 (2007), arXiv:0705.1525 [nucl-ex].
- [21] D. Androic *et al.* (G0), *Phys. Rev. Lett.* **107**, 022501 (2011), arXiv:1103.3667 [nucl-ex].
- [22] D. Balaguer Ríos *et al.*, *Phys. Rev. Lett.* **119**, 012501 (2017).
- [23] S. P. Wells *et al.* (SAMPLE), *Phys. Rev.* **C63**, 064001 (2001), arXiv:nucl-ex/0002010 [nucl-ex].
- [24] M. Gorchtein and C. J. Horowitz, *Phys. Rev.* **C77**, 044606 (2008), arXiv:0801.4575 [nucl-th].
- [25] J. Benesch *et al.* (MOLLER), (2014), arXiv:1411.4088 [nucl-ex].

- 382 [26] H. Herminghaus, A. Feder, K. H. Kaiser, W. Manz, and 389 [30] K. H. Steffens, H. G. Andresen, J. Blume-Werry,
383 H. Von Der Schmitt, Nucl. Instrum. Meth. **138**, 1 (1976). 390 F. Klein, K. Aulenbacher, and E. Reichert, Nucl. In-
384 [27] K. Aulenbacher *et al.*, Nucl. Instrum. Meth. **A391**, 498 391 strum. Meth. **A325**, 378 (1993).
385 (1997). 392 [31] A. Tyukin, Master Thesis, Inst. f. Kernphysik, JGU
386 [28] K. Aulenbacher, Eur. Phys. J. ST **198**, 361 (2011). 393 Mainz (2015).
387 [29] B. S. Schlimme *et al.*, Nucl. Instrum. Meth. **A850**, 54 394 [32] K. I. Blomqvist *et al.*, Nucl. Instrum. Meth. **A403**, 263
388 (2017), arXiv:1612.02863 [physics.acc-ph]. 395 (1998).